Prognostics Method for Analog Electronic Circuits

Arvind Sai Sarathi Vasan[1], Bing Long[2], and Michael Pecht[1]

[1]*Center for Advanced Life Cycle Engineering, University of Maryland, College Park, MD 20742, USA*
Arvind88@calce.umd.edu
pecht@calce.umd.edu

[2]*School of Automation Engineering, University of Electronic Science and Technology of China, Chengdu, China*
longbing@uestc.edu.cn

ABSTRACT

Analog electronic circuits are an integral part of many industrial systems. Failure in such analog circuits during field operation can have severe economic implications. The presence of an expert system that can provide advance warnings on circuit failures can minimize the downtime and improve the reliability of electrical systems. Through successive refinement of circuit's response to a sweep signal, features are extracted for fault prognosis. From the extracted features, a fault indicator is developed. An empirical model is developed based on the degradation trend exhibited by the fault indicator. Particle filtering approach is used for model adaptation and remaining useful performance estimation. This framework is completely automated and has the merit of implementation simplicity. The proposed framework is demonstrated on two analog filter circuits.

1. INTRODUCTION

Analog circuits are extensively used in industrial systems for implementing controllers, conditioning signals, protecting critical modules and more (Wagner & Williams, 1989). The occurrence of circuit failures during field operation will affect the system functionality and the cost of failure can be enormous (Pecht & Jaai, 2010). In most cases, these failures can be related to a fault in the system's analog circuitries, where fault refers to a change in the value of a circuit component from its nominal value which leads to a failure of the whole circuit. These faults could either be catastrophic (open and short) or parametric faults (fractional deviation in circuit components from their nominal values) (Xiao & He, 2011). For example, the degradation of electrolytic capacitors in the LC filters will cause the switching-mode power converters to fail (Chen, Wu, Chou, & Lee, 2008); an increase in resistance offered by the components within filter circuits due to the degradation of solder joints will affect the frequency band being filtered out (Brown, Kalgren, Byington & Roemer, 2007).

Prevention of circuit failures during field operation requires methods for the prediction of remaining useful performance (RUP) of the failing circuit (Lall, Bhat, Hande, More, Vaidya, & Goebel, 2011) where RUP refers to the remaining time that the circuit performance guarantees system operation. Most of the related research for analog circuits has aimed at diagnosing faults in circuits. However, no method has been suggested for predicting the remaining time till circuit failure.

In this paper, a new prognostics framework for analog circuits is proposed, aiming at "in-circuit" real-time RUP estimation. A fault indicator (FI) reflecting the evolution of fault in any of the circuit's critical component is developed. Then a model adaptation scheme using particle filters (PFs) is devised for tracking the FI and predicting the circuit's RUP.

2. PROGNOSTICS FRAMEWORK

Developing PHM strategies for analog circuits is a challenging task because of the unavailability of fault models (Aminian & Aminian, 2002). This makes the application of data-driven techniques appealing, as this does not require knowledge on material properties, structures, or failure mechanisms. An overview of the proposed prognostics framework is shown in Figure 1.

2.1. Feature Extraction

For analog circuits, the behavioral characteristics are assumed to be embedded in the time and frequency response. Hence, a test signal must be chosen such that this response can be generated and captured. Hence, we suggest the use of a sweep signal containing a frequency bandwidth larger than that of the CUT.

Arvind Sai Sarathi Vasan et al. This is an open-access article distributed under the terms of the Creative Commons Attribution 3.0 United States License, which permits unrestricted use, distribution, and reproduction in any medium, provided the original author and source are credited.

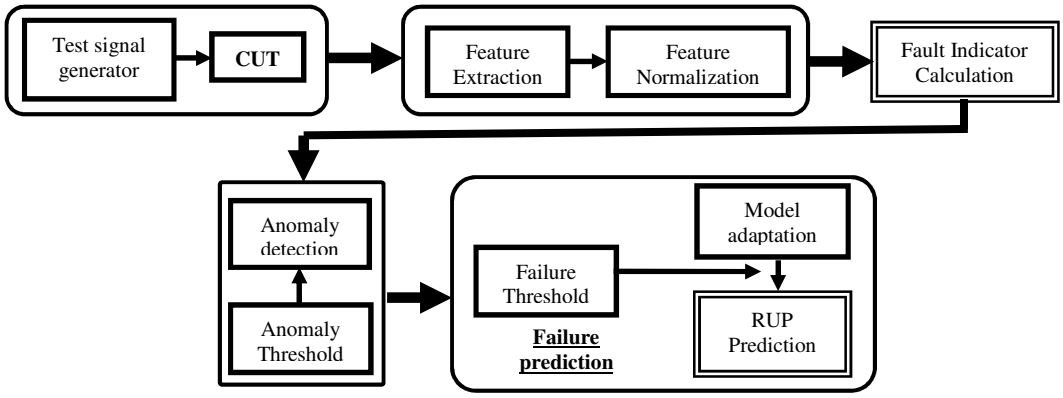

Figure 1. Overview of the proposed prognostics framework for analog electronic circuits.

This ensures that the CUT is excited by all the frequency components it is sensitive to. Also, this method allows us to acquire data at a sampling rate that depends on the CUT's bandwidth. Simple and cost effective digital forms of a sweep signal generator have been implemented with TTL logic and thus, can be incorporated on-board for testing.

From the CUT response to sweep signal, two types of features are extracted, which we call the wavelet and statistical features.

Fourier transformation is commonly used for extracting information embedded in a signal. However, Fourier transformation is suitable only for the analysis of stationary signals. A change in time of a non-stationary signal spreads over the entire frequency domain, which will not be detected through Fourier transformation. This is a drawback for fault diagnosis, as the signals to be analyzed contain time-varying frequencies. In contrast, wavelet analysis can reveal signal aspects such as trends, break points, and discontinuities. Hence, we choose wavelet features for RUP estimation in analog circuits.

In wavelet analysis, the signal's correlation with families of functions that are generated based on the shifted and scaled version of a mother wavelet $\psi(t)$ is calculated and used to map the signal of interest to a set of wavelet coefficients that vary continuously over time. The discrete version of the wavelet transform consists of sampling the scaling and shifted parameters, but not the signal or the transform. This makes the time resolution good at high frequencies, and the frequency resolution becomes good at low frequencies.

In this work, through discrete wavelet transformation, we decompose the response of the CUT stimulated by a sweep signal into the approximation and detail signals using multirate filter banks. The information contained in the response is represented using features extracted by computing the energy contained in the detail coefficients at various levels of decomposition. This is expressed as follows:

$$E_j = \sum_k \left| d_{j,k} \right|^2 ; \qquad j = 1{:}J \tag{1}$$

where and $d_{j,k}$ are the energy and k^{th} detail coefficient at j^{th} level of decomposition respectively.

The second set of features extracted includes the kurtosis and entropy of the CUT's response. Kurtosis is a statistical property which is defined as the standardized fourth moment about the mean. It provides a measure on the heaviness of the tails in the probability density function (PDF) of a signal, which is related to the abrupt changes in the signal having high values and appearing in the tails of the distribution. Kurtosis is mathematically described as follows:

$$kurt(x) = \frac{E\left[x - E[x]\right]^4}{\left[E\left[x - E[x]\right]^2\right]^2}. \tag{2}$$

On the other hand, entropy provides a measure of the information capacity of a signal, which denotes the uncertainty associated with the selection of an event from a set of possible events whose probabilities of occurrences are known. It is defined for a discrete-time signal as:

$$H(x) = -\sum_i P(x = a_i) \log P(x = a_i) \tag{3}$$

where, a_i are the possible values of x, and $P(*)$ are the associated probabilities.

2.2. Fault Indicator

When implementing prognostics at a component level, generally a fault indicator (FI) parameter is identified to monitor the degradation of the component in real-time. This parameter (e.g., the ON state V_{CE} of an IGBT (Patil, Celaya, Das, Goebel, & Pecht, 2009) and the RF impedance for interconnects (Kwon, Das & Pecht, 2010)) is chosen based on an understanding of the degradation process. From this perspective, multiple parameters corresponding to all the critical components/sub-systems need to be monitored and

processed in real-time to perform system level prognostics. This is not possible in applications like analog circuits, where there is a constraint on the available resources. So as to address this challenge, we have developed a method to construct a FI to represent circuit degradation. Here, circuit degradation refers to the degradation in any of the circuit's critical component which leads to the deviation of component's value from its nominal value. The procedure for calculating the FI is based on the well-known Mahalanobis Taguchi methodology (Taguchi & Jugulum, (2002), Soylemezoglu, Jagnnathan, & Saygin (2010)).

The FI calculation starts with the collection of the two feature sets (wavelet and statistical features). For both the feature sets, two individual Mahalanobis spaces (MSs) are constructed using their normalized feature elements and correlation coefficients.

Let $\bar{F}^1 = \{f_1^1, f_2^1, .., f_l^1\}$ and $\bar{F}^2 = \{f_1^2, f_2^2\}$ denote the wavelet and statistical features respectively, where $f_i^1; i = 1{:}\,l$ denotes the energy of the detail coefficients at the i^{th} decomposition level, l is the number of decomposition levels, and f_1^2 and f_2^2 are the kurtosis and entropy of the CUT's response. A data set formed using the feature set $[\bar{F}_j^1, \bar{F}_j^2]; j = 1{:}\,n$ with n observations made during the no fault condition is used as training data.

The mean and standard deviation of each feature element is calculated using the training data, from which the training feature sets in the no fault condition are normalized:

$$Z_{i,j}^1 = \frac{f_{i,j}^1 - \bar{x}_i^1}{s_i^1} \text{ and } Z_{k,j}^2 = \frac{f_{k,j}^2 - \bar{x}_k^2}{s_k^2}; \quad i = 1{:}\,l; k = 1{,}2; j = 1{:}\,n \quad (4)$$

where

$$\bar{x}_i^1 = \frac{\sum_{j=1}^n f_{i,j}^1}{n}, \bar{x}_k^2 = \frac{\sum_{j=1}^n f_{k,j}^2}{n}, s_i^1 = \left(\frac{\sum_{j=1}^n (f_{i,j}^1 - \bar{x}_i^1)^2}{n-1}\right)^{1/2},$$

$$\text{and } s_k^2 = \left(\frac{\sum_{j=1}^n (f_{k,j}^2 - \bar{x}_k^2)^2}{n-1}\right)^{1/2}. \quad (5)$$

After normalizing the feature sets, the Mahalanobis distances (MDs) are calculated during the no fault condition using the following mathematical expressions:

$$\mathrm{MD}_j^1 = C^{-1}\left(Z_{i,j}^1\right)^T \left(\Sigma^1\right)^{-1} \left(Z_{i,j}^1\right) \text{ and}$$
$$\mathrm{MD}_j^2 = C^{-1}\left(Z_{k,j}^2\right)^T \left(\Sigma^2\right)^{-1} \left(Z_{k,j}^2\right) \quad (6)$$

where Σ^1 and Σ^2 represents the correlation matrices for the wavelet and statistical features respectively, and are calculated from the normalized feature sets as:

$$\Sigma_{i,j}^1 = \frac{1}{n-1}\sum_{m=1}^n Z_{i,m}^1 Z_{j,m}^1 \text{ and } \Sigma_{i,j}^2 = \frac{1}{n-1}\sum_{m=1}^n Z_{i,m}^2 Z_{j,m}^2 \quad (7)$$

where C denotes the total number of fault conditions, including the no fault condition.

In order to validate the MS, observations that fall outside the normal/no fault group are identified, and the corresponding MD values are calculated. The characteristics of the abnormal group are normalized using the mean and standard deviation of the corresponding characteristics in the no fault group. The correlation matrix corresponding to the no fault group is used to compute the MDs of the faulty conditions. If the MS is constructed properly, then the MDs under the fault conditions should have higher values than the normal group. Thus, if we plot the MD values obtained from the two feature sets on a two dimensional plane, the fault conditions should be separable from the no fault condition, as shown in Figure 2. The figure also illustrates a typical trajectory in the two dimensional space representing circuit degradation.

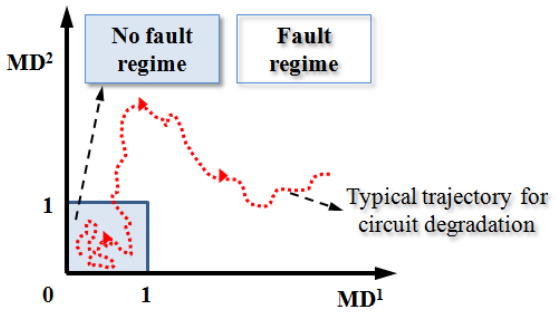

Figure 2. Illustration of fault propagation on the MS.

From Figure 2 it seems like one can observe the trajectory on the MS to understand circuit degradation. However, monitoring the trajectory in the 2D MS alone for prognostics has two drawbacks: 1) it is difficult to define a failure threshold, and 2) there can be abrupt changes in any of the MD values which are not easy to track. These drawbacks occur because of the difference in dynamic ranges for the MD values obtained from feature sets $\bar{F}^1$ and $\bar{F}^2$ (for example, for the sample circuit shown later, the range for MD^1 is found to be around 0~10^6, and for MD^2 it is found to be around 0~500). This happens because of the difference in the number of feature elements present in each of the feature sets. To address this issue, we have built a FI that gives equal weight to the MD values obtained from different feature sets.

Once the MD values are calculated for the two feature sets, the FI is computed using the following transformation:

$$\wp_j = \frac{\left(\mathrm{MD}_j^1\right)^{\frac{1}{n_1}}\left(\mathrm{MD}_j^2\right)^{\frac{1}{n_2}}}{\left(\mathrm{MD}_j^1\right)^{\frac{1}{n_1}} + \left(\mathrm{MD}_j^2\right)^{\frac{1}{n_2}}}; j = 1{,}2.. \quad (8)$$

where n_1 and n_2 represents the number of feature elements in feature sets $\bar{F}^1$ and $\bar{F}^2$ respectively. The advantage of the FI defined above is that, it is invariant to abrupt changes in MD values. This is realized by scaling it using the number of elements present in each feature set. Our study indicates that the FI has an increasing trend with respect to the amount of deviation in the faulty component from its nominal value.

In the future, new feature sets might be suggested for fault diagnosis and prognosis of analog circuits. Even if new feature sets are proposed, the above suggested FI calculation method can still be made compatible by extending Eq. (8) as follows:

$$\wp_j = \frac{\left(\mathrm{MD}_j^1\right)^{\frac{1}{n_1}}\left(\mathrm{MD}_j^2\right)^{\frac{1}{n_2}}\ldots\left(\mathrm{MD}_j^r\right)^{\frac{1}{n_r}}}{\left(\mathrm{MD}_j^1\right)^{\frac{1}{n_1}}+\left(\mathrm{MD}_j^2\right)^{\frac{1}{n_2}}+\cdots+\left(\mathrm{MD}_j^r\right)^{\frac{1}{n_r}}}; j = 1,2.. \quad (9)$$

where r denotes the total number of feature sets extracted, and n_i and MD^idenotes the total number of feature elements and the MD values corresponding to the feature set i, respectively.

2.3. Anomaly Detection Threshold

A threshold for anomaly detection using the MT method is traditionally defined as MD = 1. Here, in the calculation of the FI, a MD of 1 for both the feature sets would result in a FI value of 0.5. According to the MT method, the circuit is supposed to be displaying abnormal behavior when the FI value reaches 0.5. The interesting aspect of our study was that whenever the FI value crossed 0.5, the faulty component was found to just vary outside its tolerance range. Thus, a value of 0.5 for the FI is used as the threshold for anomaly detection.

3. FAILURE PROGNOSIS USING PFS

Failure prognosis is often performed by generating long-term predictions of FI signal until a predetermined failure threshold is reached (Orchard & Vachtsevanos, 2009). Since uncertainty is inherent to such prediction processes, the evolution of the FI is generally modeled as a stochastic process, and estimates of the RUP is made in the form of PDFs. For this purpose, stochastic nonlinear filters have garnered a lot of interest among the research community. The procedure for estimating RUP using stochastic filters involves estimation of the current health state of the system, and then performing *p*-step predictions on the future health state. These two steps are discussed next in the following subsections.

3.1. Particle Filters

One of the most commonly used forms of approximate nonlinear filters in the PHM arena is the Particle Filter (PF). Many variations of the PF are available. However, we shall focus on the sampling and importance resampling (SIR) form of the PF. The idea behind the PF is that the posterior PDF is represented by a set of random samples with associated weights $\{x_{0:k}^{(i)}, w_k^{(i)}\}_{i=1}^N; w_k^{(i)} \geq 0, \forall k$ and the Bayesian estimates are computed based on these samples (or particles) and their weights:

$$\sum_{i=1}^N w_k^{(i)}\delta\left(x_k - x_k^{(i)}\right) \xrightarrow[N\to\infty]{} p(x_k|z_{1:k}) \quad (10)$$

where $\delta(*)$ is the Dirac delta function. In practice, $p(x_k|z_{1:k})$ is usually not known. Hence, the samples $x_{0:k}^{(i)}$ are chosen from the importance density $q(*)$ and their associated (normalized, such that $\sum_i w_k^{(i)} = 1$) weights are chosen using the principle of importance sampling, which is expressed as:

$$w_k^{(i)} = \frac{p\left(z_k|x_k^{(i)}\right)p\left(x_k^{(i)}\right)}{q\left(x_k^{(i)}|z_{1:k}\right)}. \quad (11)$$

If the importance density function is chosen to be $q\left(x_k^{(i)}|x_{k-1}^{(i)}, z_{1:k}\right) = p\left(x_k^{(i)}|x_{k-1}^{(i)}\right)$ then the weights can be updated using the following relation:

$$w_k^{(i)} = w_{k-1}^{(i)}p\left(z_k|x_k^{(i)}\right). \quad (12)$$

Resampling is used to address issues introduced by the degeneracy of particles, where after a few iterations all but one particle have negligible weights. During resampling particles with small weights are eliminated, allowing us to concentrate on the particles with larger weights.

3.2. RUP Estimation

When the threshold for anomaly has been reached, the *p*-step prediction is generated. However, during the prediction process the weights of the samples are kept constant and are not updated as there are no measurements. At each prediction step, the predicted health state is checked with the failure threshold. The prediction time at which the FI crosses the failure threshold denotes the time at which the system is predicted to fail. RUP estimate is then obtained by computing the distance between the predicted time of failure and the current time instant. The PDF for RUP is obtained by finding the RUP for all the *N* paths traversed by the *N*-particles, and then associating them with their weights. We can approximate a prediction distribution (*p*-steps forward) as follows:

$$p\left(x_{k+p}|z_{1:k}\right) \approx \sum_{i=1}^N w_k^{(i)}\delta\left(x_{k+p}^{(i)}\right)dx_{k+p}. \quad (13)$$

4. RESULTS AND DISCUSSION

In this section, we demonstrate our PHM framework on two analog circuits. A Sallen-Key band-pass filter centered at 25 kHz and a biquad low-pass filter with a 10 kHz upper cut-off frequency are the sample circuits built to examine our approach (Figure 3). The circuit elements have a tolerance range of 10%. Features extracted when all the components vary within their tolerance range belong to the no-fault (NF) class. Faulty responses are obtained when any of the critical components vary beyond their tolerance range.

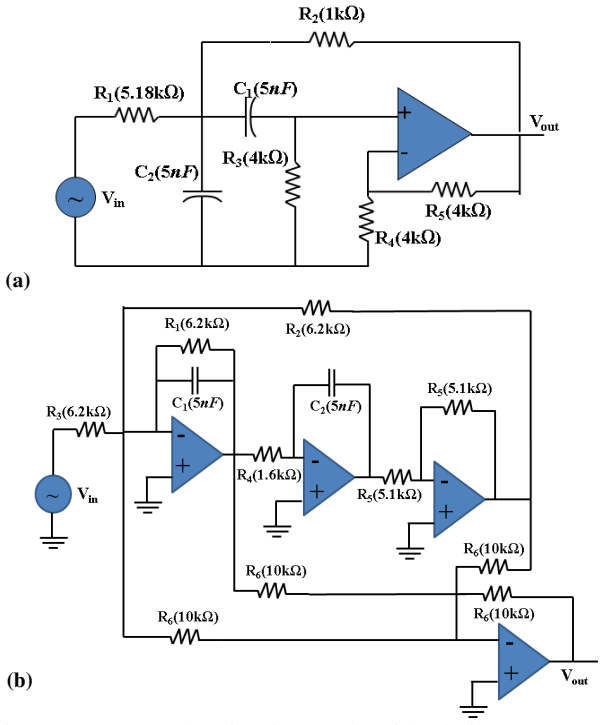

Figure 3. Sample circuits used with their component's nominal value (a) 25 kHz Sallen-Key band-pass filter and (b) biquad low-pass filter with an upper cut-off frequency of 10 kHz.

Component degradation is accompanied by a gradual change in component value (might increase or decrease). This change can have a significant impact on the circuit performance. In Section 2, the FI was developed to denote the degradation in analog circuits. Figure 4 shows the trend exhibited by the FI as the components C2 and R3 of Sallen-Key band-pass filter, and C1 and R4 of the Biquad-low pass filter, deviates from their nominal value. Here, we assume that the fault level increases gradually with respect to time, where, with each time index, the fault level increases by 0.4%. In this context, time index refers to one cycle where a 100 msec test signal stimulates the CUT and the response is measured. Through curve fitting on the FI data (obtained from features extracted during different simulated fault conditions – simulation performed using PSPICE), it is found that a model of the following form can describe the FI trend of different components in different analog circuits well:

$$\wp_{t_k} = a_{t_k}^{(1)}\left[-\left(\frac{t_k - b_{t_k}^{(1)}}{c_{t_k}^{(1)}}\right)^2\right] + a_{t_k}^{(2)}\left[-\left(\frac{t_k - b_{t_k}^{(2)}}{c_{t_k}^{(2)}}\right)^2\right] \quad (14)$$

where $\wp$ is the FI, t_k is the time index; and $a_{t_k}^{(1)}, b_{t_k}^{(1)}, c_{t_k}^{(1)}, a_{t_k}^{(2)}, b_{t_k}^{(2)}$ and $c_{t_k}^{(2)}$ are the model parameters.

In order to perform prognosis, the above regression model is exploited. However, to deal with the uncertainties caused by component tolerances and usage conditions, the model is assumed to be stochastic. Hence, the parameters of the model are subjected to Gaussian distribution. This stochastic model is fed into the online prognostics routine. Features extracted from the circuit's response are used to calculate the current FI value. This is used to estimate the model parameters. Once the diagnostic routine detects an anomaly, it triggers the prognostics module. Here, the above model's parameters are incorporated as the elements of a state vector.

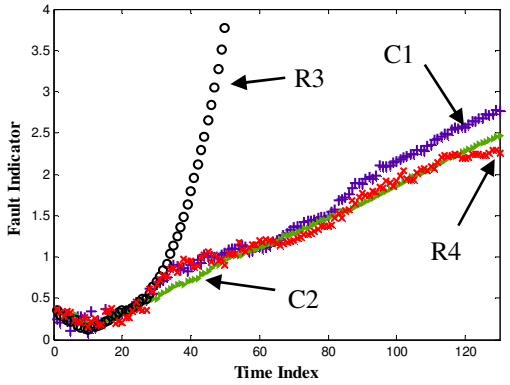

Figure 4. Trend exhibited by FI during the degradation of circuit components.

Thus, the stochastic model is a simple random walk that is employed to estimate the model parameters:

$$\left.\begin{aligned} a_{t_k}^{(1)} &= a_{t_{k-1}}^{(1)} + \omega_{1,k};\ \ \omega_{1,k}\sim N(0,\sigma_1) \\ b_{t_k}^{(1)} &= b_{t_{k-1}}^{(1)} + \omega_{2,k};\ \ \omega_{2,k}\sim N(0,\sigma_2) \\ c_{t_k}^{(1)} &= c_{t_{k-1}}^{(1)} + \omega_{3,k};\ \ \omega_{3,k}\sim N(0,\sigma_3) \\ a_{t_k}^{(2)} &= a_{t_{k-1}}^{(2)} + \omega_{4,k};\ \ \omega_{4,k}\sim N(0,\sigma_4) \\ b_{t_k}^{(2)} &= b_{t_{k-1}}^{(2)} + \omega_{5,k};\ \ \omega_{5,k}\sim N(0,\sigma_5) \\ c_{t_k}^{(3)} &= c_{t_{k-1}}^{(3)} + \omega_{6,k};\ \ \omega_{6,k}\sim N(0,\sigma_6) \end{aligned}\right\} \quad (15)$$

$$\wp_{t_k} = a_{t_k}^{(1)}\left[-\left(\frac{t_k - b_{t_k}^{(1)}}{c_{t_k}^{(1)}}\right)^2\right] + a_{t_k}^{(2)}\left[-\left(\frac{t_k - b_{t_k}^{(2)}}{c_{t_k}^{(2)}}\right)^2\right] + \varepsilon_k;\ \varepsilon\sim N(0,\sigma_\varepsilon)$$

where $\wp_{t_k}$ is the measured value of the FI variable at time index t_k, and $N(0,\sigma)$is a Gaussian distribution with mean zero and standard deviation σ. Using the PFs, a p-step prediction can be made on the model parameters, with which the future values of the FI can be calculated. The RUP is calculated based on the time index at which the predicted FI value crosses the failure threshold. In on our study, we found that by the time the FI value reaches a value of 2, the fault level for the most of the components has crossed 40%. Hence, in this work we have chosen a value of 2 for the FI as the failure threshold. This is just a qualitative threshold. In the future, a method to establish a failure threshold needs to be investigated. Also, the initial values of the model parameters (used from the curve fitting) and their

standard deviations are assumed to be known here for the sake of simplicity. In practice, an efficient method needs to be devised to choose these values for the model parameters.

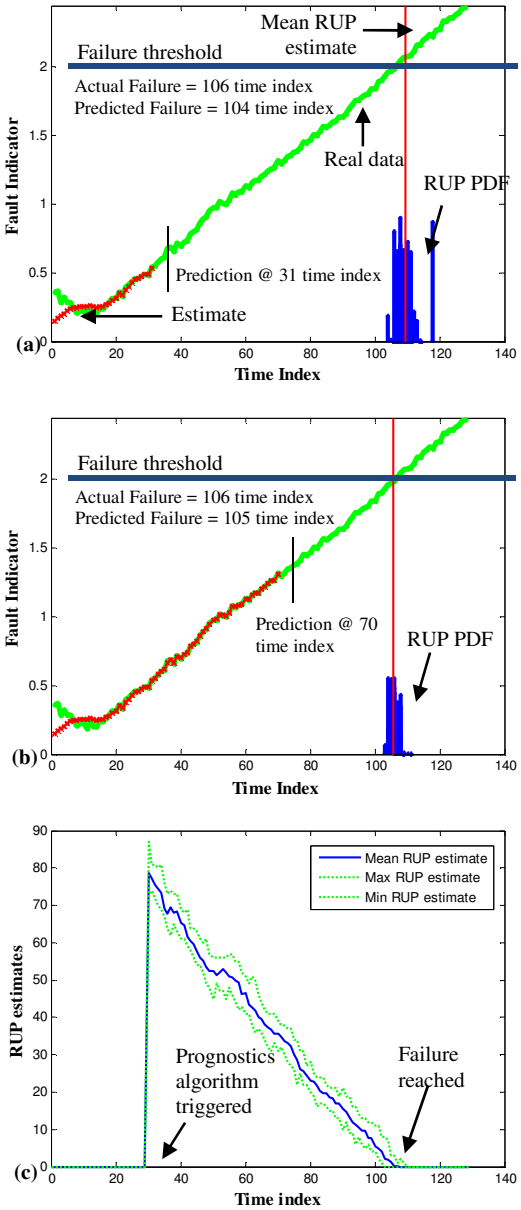

Figure 5. Prognostics results using particle filters for the Sallen-Key band-pass filter for fault progression in component C2 (a) Prediction result at time index 31, (b) Prediction result at time index 70, and (c) RUL estimation at every time index.

The results for fault progression in component C2 of the Sallen-Key band-pass filter circuit is shown in Figure 5. Figure 5(a) shows the RUP estimation at the time instant an anomaly was detected (i.e., $\wp > 0.5$). This occurred at time index 31. Thus, the data from the first 31 time indices alone are used to update the model. The estimated RUP is 73 and thus the predicted end-of-life (EOL) is 104, and the actual failure occurs at the 106th time index. In Figure 5(b), the prognostics results performed at time index 70 are shown. Now, the predicted EOL is the 105th time index. Thus, the error in prediction is only one. Also, the prediction PDF becomes narrower as we get closer to the failure time indicating the improvement in prediction confidence. Figure 5(c) shows the RUP estimates at different time indices with 95% confidence bounds.

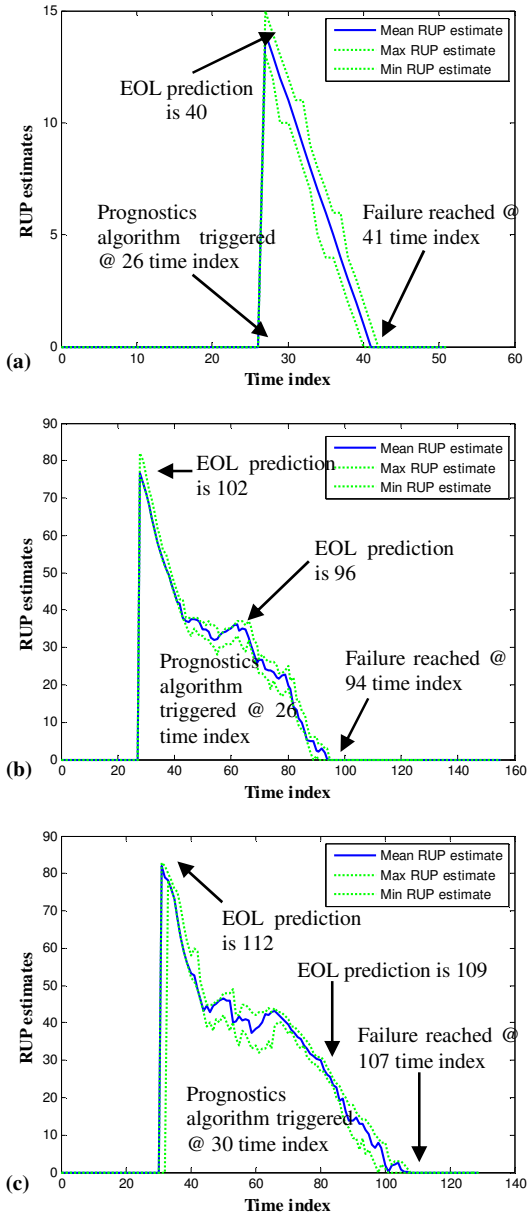

Figure 6. Prognostic results using particle filters for (a) Sallen-Key band-pass filter for fault progression in component R3, (b) biquad low pass filter for fault progression in component C1, and (c) biquad low pass filter for fault progression in component R4.

In order to show the applicability of the proposed approach for different components and circuits, the RUP estimation at different time indices for the component R3 in the Sallen-Key band-pass filter circuit, and the components C1 and R4 for the biquad low-pass filter circuit are shown in Fig. 6.

5. CONCLUSION

Existing test strategies for analog circuits are useful only after a failure has occurred. However, the nature of functions performed by industrial system demands test strategies that would enable the prevention of circuit failures. To address this concern, a prognostics framework for analog circuits is proposed in this paper.

The prognostics module includes a new fault indicator (FI) and a model adaptation scheme to track the evolution of FI. One feature of the FI is its ability to summarize the degradation level in any of the circuit's critical component. This allows RUP estimation to be performed without monitoring the individual components of the circuit leading to the reduction in resources needed for prognostics. Another feature of the FI is its compatibility to future changes in the extracted features. Thus, even if new features are introduced in the future, RUP predictions can be obtained from the circuit's response.

The model adaptive ability of the prognostic routine enables the real-time prediction of the circuit's RUP even under the presence of uncertainties that are introduced by component tolerances and time varying nature of the environment. Since this method involves a statistical approach for RUP prediction, the RUP estimate is given in the form of probability distributions, indicating the confidence levels in the prediction. Thus, preventive maintenance actions can be performed using the estimated RUP information for avoiding unexpected system failures due to faults in circuits.

ACKNOWLEDGEMENT

The authors would like to thank the more than 100 companies and organizations that support research activities at the Prognostics and Health Management Group within the Center for Advanced Life Cycle Engineering at the University of Maryland annually.

REFERENCES

Aminian, F., & Aminian, M. (2002). Analog fault diagnosis of analog circuits using neural networks. *IEEE Trans. Instrum. Meas.*, vol. 51, no. 3, pp. 544-550.

Brown, D., Kalgren, P., Byington, C., & Roemer, M. (2007) Electronic prognostics – a case study using global positioning system (GPS). *Microelectron. Reliab.*, vol. 47, pp. 1874-1881.

Chen, Y-M., Wu, H-C., Chou, M-W., & Lee, K-Y. (2008). Online failure prediction of electrolytic capacitors for LC filter of switching-mode power converters. *IEEE Trans. Ind. Electron.,* vol. 55, no. 1, pp. 400-406.

Kwon, D., Azarian, M., & Pecht, M. (2010). Prognostics of interconnect degradation using RF impedance monitoring and sequential probability ratio test. *International Journal of Performability Engineering*, vol. 6, no. 5, pp. 443-452.

Orchard, M. & Vachtsevanos, G. (2009). A particle-filtering approach for on-line fault diagnosis. *Trans. Inst. Meas. Control*, vol. 31, no., pp. 221-246.

Patil, N., Celaya, J., Das, D., Goebel, K., & Pecht, M. (2009). Precursor parameter identification for insulated gate bipolar transistor prognostics. *IEEE Trans. Reliab.*, vol. 58, no. 2, pp. 271-276.

Pecht, M. & Jaai, R. (2010). A prognostics and health management roadmap for information and electronics-rich systems. *Microelectron. Reliab.*, vol. 50, no. 3, pp. 317-323.

Soylemezoglu, A., Jagnnathan, S., & Saygin, C. (2010). Mahalanobis Taguchi system as a prognostic tool for rolling element bearing failures. *J. Manuf. Sci. Eng.*, vol. 132, no. 5, pp. 051014-1-051014-12.

Taguchi, G. & Jugulum, R. (2002) *The Mahalanobis-Taguchi strategy.* Wiley-Interscience, New York.

Wagner, K. & Williams, T. (1989). Design for testability of analog/digital networks. *IEEE Trans. Ind. Electron*., vol. 36, no. 2, pp. 227-230.

Xiao, Y. & He, Y. (2011). A novel approach for analog fault diagnosis based on neural networks and improved kernel PCA. *Neurocomputing*, vol. 74, pp. 1102-1115.